



RECONSTRUCTION OF METAL OBJECTS - 3D PHOTOGRAMMETRY AND CLAY COATING

Hasan Kemal SÜRME^{1*}


¹Istanbul University - Cerrahpasa, Department of Motor Vehicles and Transportation Technologies, 34500, Istanbul, Türkiye

Abstract: This work focuses on the development of a reconstruction process using 3D photogrammetry for metal objects, which are often difficult to scan in three-dimensional (3D) due to their shiny, smooth and featureless surfaces. Usually, expensive 3D scanning technologies are used for high accuracy reconstructions. This research presents a novel approach using clay powder to improve the geometric accuracy of 3D reconstructions through a coating process, a first in the literature. Twelve metal objects with cubic, cylindrical and spherical geometries were selected for the study. They were photographed in a controlled environment using a turntable, camera and 18-135 mm lens. 3D reconstructions of these objects were obtained initially without coating and then by applying clay powder. The reconstructions were then compared for geometric accuracy and mesh quality. The main findings from the study show that clay coating significantly improves the geometric accuracy of the reconstruction process. In addition, it also improves the homogeneity of the mesh structures. These improvements were confirmed by deviation analysis, which compared the models generated by the reconstruction process with computer-aided design (CAD) models drawn according to the actual dimensions of the objects. The study highlights the potential of clay coating as a viable alternative method to improve geometric accuracy in the 3D reconstruction process.

Keywords: 3D Photogrammetry, Coating, Computer aided design (CAD), Image based modeling, Reconstruction, Reverse engineering

*Sorumlu yazar (Corresponding author): Istanbul University - Cerrahpasa, Department of Motor Vehicles and Transportation Technologies, 34500, Istanbul, Türkiye

E mail: hksurmen@iuc.edu.tr (H.K. SÜRME)

Hasan Kemal SÜRME  <https://orcid.org/0000-0001-8045-9193>

Received: December 21, 2024

Accepted: February 05, 2025

Published: March 15, 2025

Cite as: Surmen HK. 2025. Reconstruction of metal objects - 3D photogrammetry and clay coating. BSI Eng Sci, 8(2): 507-516.

1. Introduction

Three-dimensional (3D) reconstruction is a rapidly evolving field encompassing various technologies to create precise models of physical objects. It finds extensive applications in engineering, biomedical sciences, industrial design, and manufacturing, providing efficient capture of geometric data (Reis, 2018; Javaid et al., 2021). One challenge it addresses is the scanning of free-form objects that are difficult to model using traditional 3D drafting software. Technologies such as 3D laser scanning (Yaman et al., 2017; Yang et al., 2018), computed tomography (Cansiz et al., 2014), structured light (Gessner et al., 2022), and 3D photogrammetry (Mathys et al., 2019; Surmen, 2023) each offer distinct advantages and drawbacks. However, high initial costs and specialized equipment remain significant barriers to widespread adoption (Cansiz et al., 2014; Yang et al., 2018).

3D photogrammetry is increasingly popular due to its affordability, portability, ability to capture color, and wide scanning range. Also known as image-based 3D modeling (Remondino and El-Hakim, 2006) or photo scanning (Seeberger et al., 2016), photogrammetry finds applications in diverse fields including architecture (Pepe and Costantino, 2020), engineering (Kanun, 2021), archaeology (Molnár, 2019), cultural heritage (Kingsland,

2020), medical sciences (Orun et al., 2018; Kurilová et al., 2023), forensics (Tóth et al., 2021), biomedical research (Struck et al., 2019), biology (Eulitz and Reiss, 2015), and geology (Gomez and Kennedy, 2018). This technique involves capturing multiple photographs of an object from different angles, which are then processed using specialized software to create point cloud models, triangular mesh polygon models, or photorealistic textured 3D models. However, challenges arise when dealing with objects that have shiny or reflective surfaces (Valinasab et al., 2015; Kohtala et al., 2021).

The reconstruction of metal objects, including parts and devices, using 3D scanning is crucial for applications such as reverse engineering and archival purposes in fields like engineering, biomedical sciences, and archaeology (Wang et al., 2016; Helle and Lemu, 2021). The glossy and reflective surfaces of metallic materials pose significant challenges even for advanced technologies such as structured light scanning (Surmen et al., 2018). Most 3D scanning methods rely on capturing the way light reflects off an object to create a detailed 3D model. On reflective surfaces, this process becomes problematic for a few key reasons such as specular reflection and glare. Metallic surfaces tend to reflect light in a mirror-like, specular manner, meaning the light doesn't scatter in all directions but instead reflects at specific angles. This causes the scanning system to miss important data



about the object's geometry since the reflected light might not reach the sensor or might be misinterpreted. In addition, highly reflective materials can cause glare, which overwhelms the sensor's ability to capture the correct pattern or laser light. This can lead to the sensor being "blinded" by the reflection, resulting in data loss or errors in measuring the shape of the object. Surface preparation, including the application of coatings, may be necessary to facilitate accurate scanning. Furthermore, post-processing and editing of models derived from the reverse engineering process are often required (Wang et al., 2016; Helle and Lemu, 2021). Therefore, improving the accuracy of initial 3D reconstructions can minimize subsequent editing efforts, thereby saving time, labor, and costs.

This study aims to evaluate and enhance the effectiveness of 3D photogrammetry in reconstructing metal objects. Additionally, it explores the use of clay powder as a coating material in photogrammetric modeling—an approach valued for its affordability, natural composition, ease of application, and environmental friendliness compared to commercial alternatives. Comparative analyses of clay-coated and uncoated object reconstructions focus on geometric accuracy and mesh structures. Twelve reconstructions were performed using 3D photogrammetry, and results include solid and mesh models alongside deviation analyses referencing CAD models based on actual object dimensions. Maximum and minimum geometric deviations are quantified, and 3D color maps illustrating deviation regions are presented. Ultimately, the study assesses how clay coating influences geometric accuracy and mesh structures in generated reconstructions.

2. Materials and Method

Photogrammetry enables the acquisition of dimensions, position, shape, and texture of objects through the analysis of photographs, providing both measurement data and visual information. The process of photogrammetric modeling involves several stages: planning the photography session based on the objects' shapes and geometric details, camera calibration, generation of a point cloud using specialized software, and conversion of this point cloud into solid, mesh, and textured 3D models. The fundamental principle underlying both digital close-range photogrammetry (Awange and Kiema, 2019) and aerial photogrammetry (Axelsson, 1991) is central perspective projection, illustrated in Figure 1.

Collinearity equations, which are the basic mathematical equations underlying photogrammetry, are used to unify the coordinate system of the obtained image with the object being photographed (equations 1 and 2):

$$x_p = -c \frac{r_{11}(X_p - X_0) + r_{12}(Y_p - Y_0) + r_{13}(Z_p - Z_0)}{r_{31}(X_p - X_0) + r_{32}(Y_p - Y_0) + r_{33}(Z_p - Z_0)} \quad (1)$$

$$y_p = -c \frac{r_{21}(X_p - X_0) + r_{22}(Y_p - Y_0) + r_{23}(Z_p - Z_0)}{r_{31}(X_p - X_0) + r_{32}(Y_p - Y_0) + r_{33}(Z_p - Z_0)} \quad (2)$$

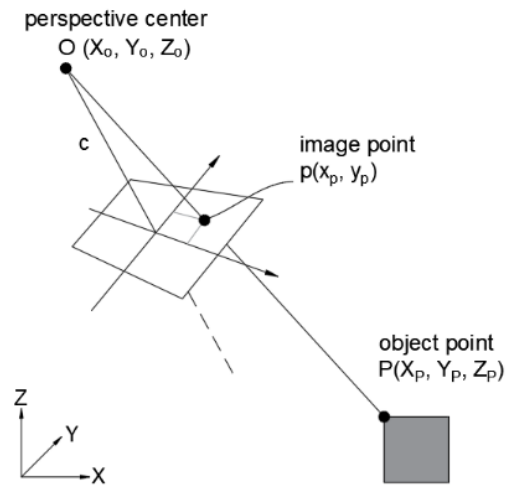


Figure 1. Principle of central perspective.

Where X_p , Y_p represent the coordinates of the image point (p); c is the calibrated focal length or also called the principal distance. X_0 , Y_0 , and Z_0 indicate the position of the perspective center in the object's space; r_{ij} for $i, j = 1, 2, 3$ are the elements of the orthogonal rotation matrix comprising the three angles ω , ϕ and κ . X_p , Y_p , Z_p are the coordinates of the object point (P). The six parameters (ω , ϕ , κ , X_0 , Y_0 , Z_0) represent the elements of exterior orientation, which define the position of the camera in space. This study employs 3D photogrammetry to investigate the reconstruction of metal objects and assess the influence of clay powder coating. The chosen objects include basic geometric shapes commonly found in mechanical parts: prisms, cylinders, spheres, and surfaces with concave and convex edges. These objects, such as cubes, cylinders, spheres, and their variants created through constructive solid geometry techniques (Ghali, 2008), serve as subjects for exploring various applications of 3D reconstruction, as illustrated in Figure 2.

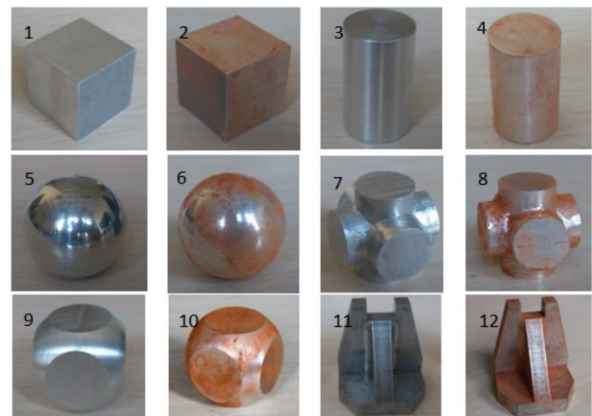


Figure 2. Uncoated and clay coated objects used in 3D photogrammetry.

In this study, aluminum metal objects were manufactured using the CNC method and subsequently prepared for accurate 3D reconstruction via

photogrammetry. The surfaces of these objects, known for their inherent shine and smoothness, posed a challenge to achieving precise reconstructions, a critical factor highlighted in prior research (Puerta et al., 2020). To address this, a novel approach was introduced wherein clay, selected for its matte texture and perceptibility, was employed as a coating material. Notably, this study marks the first use of clay for such purposes, leveraging its affordability, accessibility, safety, and ease of handling and storage over extended periods. Clay powder was used in the coating process. It was obtained from the dry form of the clay material, which was carefully pulverized. The powder was then gently applied to the surfaces manually using a soft brush. Clay coating was applied in a thin layer to surfaces for specific objects (2, 4, 6, 8, 10, and 12), thereby enhancing their perceptibility during the subsequent photographing phase. This coating process aimed to mitigate the challenges posed by shiny or transparent surfaces, thereby facilitating more accurate 3D reconstructions. The workflow of the 3D photogrammetry technique employed in this study encompassed three primary phases: photographing, uploading images to cloud-based software, and generating 3D models, as depicted in Figure 3. Each phase was meticulously executed to ensure comprehensive data acquisition and processing integrity.

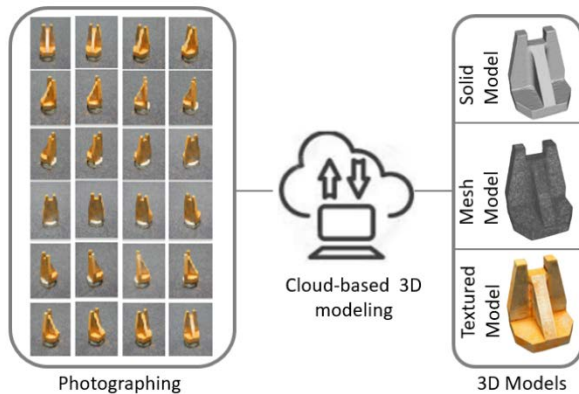


Figure 3. Stages of 3D photogrammetric modeling.

In the context of 3D photogrammetric modeling, ensuring high-quality outcomes necessitates adhering to established best practices. It is widely recommended in the literature that photographs for such applications should exhibit a minimum overlap of 60% (Matthews, 2008; Slaker and Mohamed, 2017). This overlap is crucial as it enables the software to effectively stitch together the images and maintain geometric continuity throughout the 3D model generation process. To achieve this, photographs should be captured in a manner that ensures comprehensive coverage of all surfaces of the object from various angles. Each image should overlap sufficiently with adjacent ones, facilitating robust reconstruction of the object's geometry and texture. To mitigate potential errors arising from environmental conditions or operator variability during the

photographing phase, a straightforward mechanism has been developed. This mechanism, depicted in Figure 4, serves to standardize the photographic process, thereby enhancing consistency and reliability across multiple trials or comparisons. Such procedural consistency is essential for ensuring the accuracy and reproducibility of 3D photogrammetric modeling results.

This mechanism is mounted on a fixed stand equipped with an indicator to precisely measure its rotational angle. It consists of a turntable with a pointer indicating the angle position, along with a Canon EOS 50D camera paired with an 18-135 mm lens. The photographs were taken indoors in a controlled environment devoid of natural daylight. Illumination was provided by a fluorescent light positioned above the turntable. To minimize potential reflections, both the turntable and the background were covered with dark, non-reflective fabric.

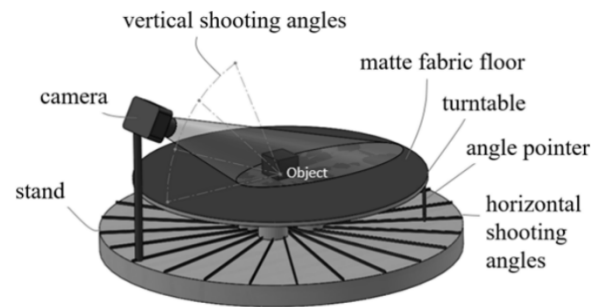


Figure 4. Stages of 3D photogrammetric modeling.

The photography methodology involved rotating the turntable approximately 15 degrees around its axis to ensure sufficient overlap (60-90%) between successive photographs. This approach draws inspiration from the photo-sculpture technique (Beaman et al., 1997), historically used to replicate objects in the 19th century. It was selected due to the limitations of capturing all geometric details of objects from a single vertical angle. Hence, photographs were taken at multiple vertical angles: one shot at a 35-degree angle, and two shots at 0 degrees and 45 degrees, respectively.

The camera was positioned approximately 40 cm away from the object, and no flash was utilized to avoid unwanted reflections. Photographs were captured at a resolution of 15.1 megapixels (4752 x 3168 pixels). Following capture, the photos were uploaded to a computer equipped with Autodesk ReCap Photo, a 3D photogrammetry software that supports cloud-based processing. The software facilitated the upload of photos to the cloud system for 3D modeling. Once processed, the resulting 3D models were downloadable in RCM (Reality Computing Mesh) format, which supports surface models. Additionally, models could be exported in various formats including OBJ, OBJ (Quads), FBX, STL, PLY, PTS, and RCS.

Mesh data reports were generated to meticulously examine the structure of the 3D mesh models. After

assessing visual accuracy, a comprehensive deviation analysis was conducted for each reconstructed object to ascertain geometric accuracy and any discrepancies. The workflow illustrated in Figure 5 guided this deviation analysis.

Initially, physical object dimensions were meticulously measured, and 3D CAD models were meticulously crafted based on these precise measurements. These CAD models served as the gold standard reference models against which the accuracy of the reconstructed 3D models was evaluated. Post-scaling the 3D reconstructed models to match the real-world objects, they underwent rigorous comparison with the CAD models using the advanced 'Difference Analysis' tool available within the ReCap software.

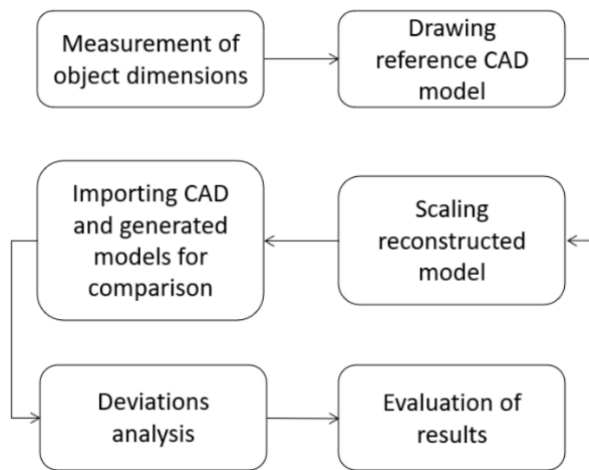


Figure 5. Workflow chart for deviation analysis.

3. Results and Discussion

3.1 Evaluation of Visual and Geometric Accuracy of the Reconstructed 3D Models

Figure 6 showcases 3D solid models reconstructed from both uncoated and clay-coated metal objects using 3D photogrammetry within the scope of this study. When examining the cube-shaped Model 1 and its clay-coated counterpart, Model 2, it is evident that Model 2 exhibits reduced surface roughness compared to Model 1. Additionally, the edges of Model 2 appear smoother and sharper.

There is a noticeable difference in shape between Model 3 and Model 4, which were generated from cylindrical metal objects. Due to the glossiness caused by their cylindrical shape, Model 3 was not accurately reconstructed. However, Model 4 shows significant improvement in geometric accuracy with the application of clay coating. The clay coating not only minimized reflections on the object's surface but also imparted a discernible texture.

Similar improvements were observed in the sphere-shaped Object 5 and its clay-coated version, Object 6.

Object 7 consists of three cylindrical parts with identical geometry along the x, y, and z axes. Despite some superficial surface issues, the 3D model of Object 7 was successfully generated. The reconstruction process was repeated with the application of clay powder to the objects, resulting in improved geometric accuracy. Objects 9 and 10 feature geometries derived from the intersection of cube and sphere shapes. It was observed that model 10 achieved higher geometric precision compared to model 9, attributed to the clay coating. Examining model 11, reconstructed from a metal machine part, revealed inaccuracies particularly in concave edges.

Following the application of clay coating and subsequent reconstruction, it was noted that concave edges could be accurately reproduced. Moreover, improvements were observed in the accuracy of edges, corners, and overall surface details of the model.

3.2 Deviation Analysis Results

Deviation analysis plays a critical role in both the numerical and visual assessment of geometric accuracy when comparing different models. In our study, we conducted deviation analysis to meticulously observe the geometric differences between models reconstructed from uncoated and clay-coated metal objects. This analysis followed the structured approach outlined in Figure 5, utilizing Autodesk ReCap Photo's 'Difference Analysis' tool.

The CAD models used for comparison were meticulously created to match the exact dimensions of the objects using CAD software, and then converted into STL format to facilitate the deviation analysis. Prior to analysis, all models were scaled to ensure alignment with the original object dimensions. A tolerance threshold of 0.2 mm was set based on the bounding box of the models, which on average enclosed objects within 125,000 mm³. The results of the deviation analysis are visualized in Figure 7, where colored zones on the models indicate deviations from the CAD models. Green zones represent areas where deviations fall within the ± 0.2 mm tolerance range, highlighting high geometric accuracy. Zones colored in shades from purple to blue signify areas where deviations exceed this tolerance. Notably, models treated with clay coating showed an increase in the proportion of green zones, indicating enhanced geometric precision. This improvement underscores the positive impact of clay coating on the accuracy of reconstructed objects across various surface types, including flat, cylindrical, and spherical geometries.

Table 1 provides a detailed summary of the maximum and minimum deviations observed in both uncoated (odd-numbered models) and clay-coated (even-numbered models) processes. Maximum deviations indicate positive geometric differences, while minimum deviations indicate negative differences.

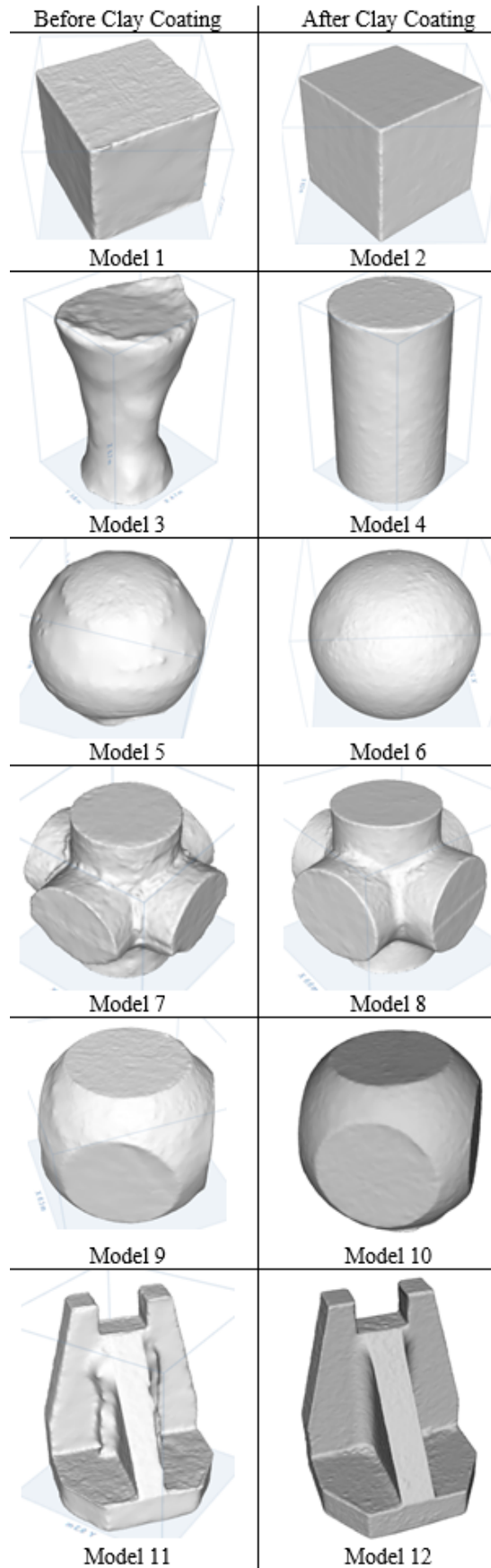


Figure 6. 3D models generated by 3D photogrammetry: The left column shows the 3D models reconstructed without the clay-coating process. The right column shows the 3D models reconstructed with the clay coating process.

Both the graphical representation in Figure 7 and the tabulated data in Table 1 demonstrate a significant reduction in both maximum and minimum deviations with the application of clay coating. Furthermore, the spread and magnitude of deviations across the surfaces of the models were notably reduced, indicating overall improvement in geometric fidelity.

The clay coating process also contributed to smoother and more accurately defined edges in all models, with particularly noticeable benefits in cylindrical and spherical surfaces. Moreover, it effectively addressed significant negative deviations observed on concave edges, further highlighting its role in enhancing geometric accuracy.

In conclusion, our study illustrates that clay coating not only minimizes surface reflections but also enhances the geometric accuracy of reconstructed 3D models. This improvement is evident across a variety of object geometries and underscores the efficacy of clay coating in advanced 3D photogrammetry applications.

Table 1. Maximum and minimum deviations of the reconstructed objects

Model No	Max. Deviation (mm)	Min. Deviation (mm)
1	1.8382	-0.6253
2	0.1491	-0.2530
3	2.9515	-2.1976
4	0.3177	-0.4748
5	1.8390	-0.6571
6	0.7467	-0.3313
7	1.3446	-0.5016
8	0.6259	-0.3205
9	1.2879	-0.7724
10	0.4671	-0.3819
11	1.0938	-2.1024
12	0.7072	-0.6389

3.3 Mesh Structure

In the study, 3D mesh models were generated for each metal object. These models are triangular polygon models that contain vertex, edge, and face data.

The 3D mesh models also provide information about the mesh structures of the models, their density, and their homogeneity. As the mesh homogeneity increase, the quality of the reconstruction also increases and the 3D model more accurately represents the object geometry (Rues et al., 2021).

The quality of the mesh structure becomes more important in ensuring dimensional accuracy, especially for objects with curved surfaces. Images of mesh models are shown in Figure 8. The difference in mesh structure between models generated from coated and uncoated objects can be clearly seen. In addition, the mesh reports for each model, containing the number of vertices and faces, are shown in Table 2.

When the mesh models of each object are examined, it is

generally observed that the clay coating process homogenizes the mesh structures. The heterogeneous mesh structures are generally observed on the models generated from uncoated objects. It is seen that the mesh structures become denser at the edges and corners.

Table 2. Mesh reports of the reconstructed objects

Model No	Vertice Number	Face Number
1	35.646	64.740
2	20.204	35.478
3	13.609	24.106
4	18.758	34.144
5	25.074	43.018
6	32.448	57.282
7	36.591	63.536
8	48.233	83.072
9	32.867	58.148
10	20.273	35.198
11	69.680	125.482
12	61.217	111.500

The clay coating process reducing the glossiness of the surfaces also provided a featured texture to the surfaces. Thus, homogeneity has improved along with the geometric accuracy of the edges and surfaces.

The mesh reports of the models presented in Table 2 showed that while the clay coating increased the homogeneity, it decreased the mesh element numbers for some models.

Considering the mesh model obtained after the clay coating process of object 1, it was determined that the number of vertices decreased from 35.646 to 20.204, and the number of faces decreased from 64.740 to 35.478. Thereby, it can be said that the clay coating reduces the number of vertices by 43% and the number of faces by 45% for object 1.

Considering models 9 and 10, it is seen that the number of vertices has decreased from 32.867 to 20.273 and the number of faces has decreased from 58.148 to 35.198 after the clay coating process. Thereby, the number of vertices decreased by 38%, and the number of faces decreased by 39% for object 5.

Considering models 11 and 12, it is seen that the number of vertices has decreased from 69.680 to 61.217 and the number of faces has decreased from 125.482 to 111.500 after the clay coating process. Thereby, the number of vertices decreased by 12%, and the number of faces decreased by 11% for object 6.

However, for objects 2, 3, and 4 the coating process increased the number of mesh elements. Within the scope of these results, it may be said that the clay coating causes an increase in the number of mesh elements in models with curved, cylindrical, and spherical surfaces, and a decrease in models with flat surfaces. It is understood that both effects in the number of mesh elements are a result of the clay coating increasing the geometric accuracy.

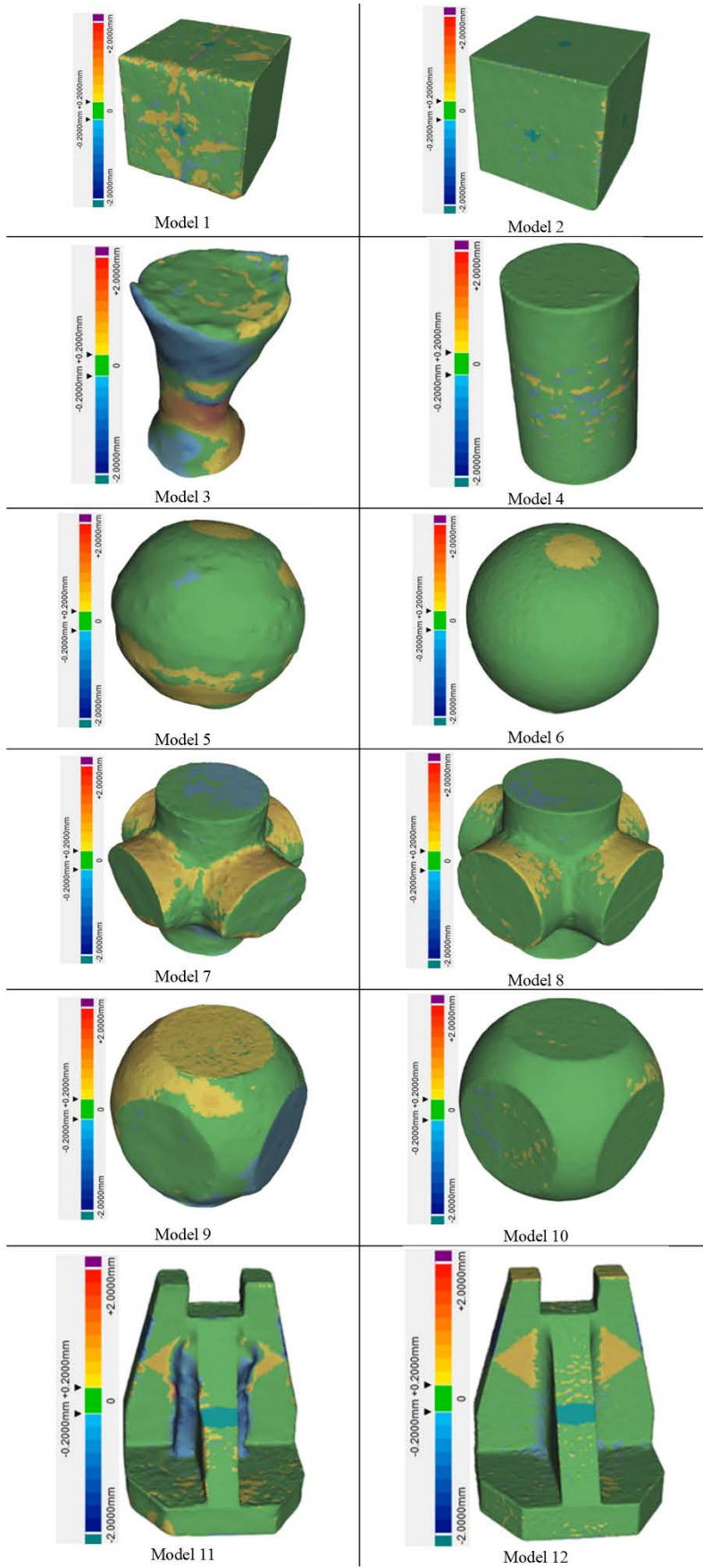


Figure 7. Results of difference analysis of the models: The left column shows the 3D models reconstructed without the coating process. The right column shows the 3D models reconstructed with the clay-coating process. Notice how the clay coating process increases the green areas within 0.2mm tolerances.

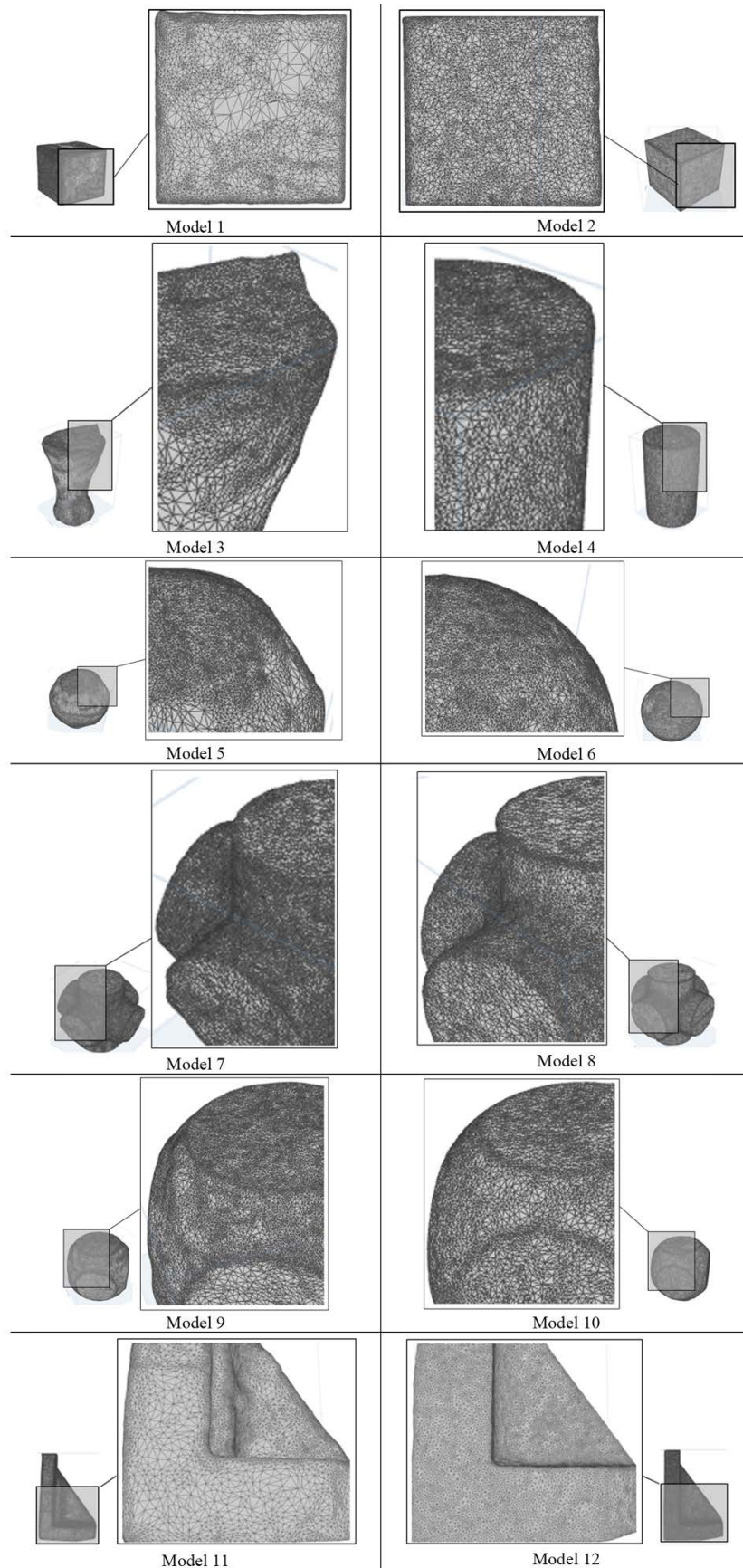


Figure 8. Mesh structures of reconstructed metal objects: The left column shows the mesh structures of the models reconstructed without the coating process. The right column shows mesh structures of the models reconstructed with the clay-coating process. Notice how the clay coating process improves mesh homogeneity in addition to improving model geometry.

This study has some limitations. The coating process was performed manually. The coating was made using clay powder obtained from the dry form of the clay material. The clay powder was crushed as much as possible. The powder was then applied in a thin layer to the surfaces using a soft brush. The objects used in the study, in addition to being metallic, have polished and very smooth surfaces. The adhesion of the clay powder was more difficult on cylindrical and spherical surfaces. The fineness of the powder enhanced the coating ability. No chemicals were used in this study to either aid in the adhesion of the powder to the surface or as part of the coating material. The clay powder can be coated using a spraying device, and coating performance can be observed. The metal objects included in the study were selected from various objects with prismatic, cylindrical, and spherical shapes to observe the effects of geometric differences accordingly. Although the reconstructed objects have various shapes, they are not very geometrically detailed objects. The photographs were taken in a closed environment to isolate external factors for the comparisons. The contribution of the clay coating to the outdoor 3D photogrammetry applications can be evaluated by the daylight applications.

4. Conclusions

This study introduced and evaluated the novel application of the clay coating process in conjunction with 3D photogrammetry for reconstructing metal objects with diverse geometric surfaces. The findings clearly demonstrate that the clay coating process significantly enhances the geometric accuracy and mesh structure of 3D models compared to uncoated objects. Both solid models and deviation analyses confirm marked improvements in edge definition, corner sharpness, and overall surface fidelity due to clay coating. Notably, the process reduces geometric deviations, evidenced by minimized maximum and minimum deviations and fewer instances of deviations beyond tolerance thresholds. Moreover, the impact on mesh structure was notable, with a reduction in irregularities and a more uniform mesh pattern observed post-coating. Clay, being a natural, cost-effective material with light-absorbing properties and a tactile texture, effectively enhances reconstruction outcomes and dimensional precision. The integration of clay coating with 3D photogrammetry presents a viable alternative to expensive 3D scanning techniques characterized by high initial costs and limited flexibility. This approach not only offers enhanced accuracy but also expands the accessibility of high-quality 3D reconstruction to diverse applications. Future research may further explore optimization strategies and broader applicability of this combined method in various fields requiring precise geometric modeling.

Author Contributions

The percentages of the author' contributions are presented below. The author reviewed and approved the final version of the manuscript.

Table with 2 columns: Author, H.K.S. Values: C=100, D=100, S=100, DCP=100, DAI=100, L=100, W=100, CR=100, SR=100

C=Concept, D= design, S= supervision, DCP= data collection and/or processing, DAI= data analysis and/or interpretation, L= literature search, W= writing, CR= critical review, SR= submission and revision.

Conflict of Interest

The author declared that there is no conflict of interest.

Ethical Consideration

Ethics committee approval was not required for this study because of there was no study on animals or humans.

References

Awange J, Kiema J. 2019. Fundamentals of photogrammetry, environmental geoinformatics. Springer, Cham, Germany, pp: 161-178.
Axelsson P. 1991. Fundamentals of real-time photogrammetry, ISPRS J Photogrammet Remote Sens, 46(2): 114-115.
Beaman JJ, Barlow JW, Bourell DL, Crawford RH, Marcus HL, McAlea KP. 1997. Polymers in solid freeform fabrication, solid freeform fabrication: A new direction in manufacturing. Springer, Boston US.
Cansiz E, Arslan YZ, Turan F, Atalay B. 2014. Computer-assisted design of patient-specific sagittal split osteotomy guide and soft tissue retractor. J Medic Biol Eng, 34(4): 363.
Eulitz M, Reiss G. 2015. 3D reconstruction of SEM images by use of optical photogrammetry software. J Struct Biol, 191(2): 190-196.
Gessner A, Ptasiński W, Adam W. 2022. Accuracy of the new method of alignment of workpiece using structural-light 3D scanner. Advan Sci Technol Res J, 16(1): 1-14.
Ghali S. 2008. Constructive solid geometry, Introduction to geometric computing. Springer, London, UK, pp: 277-283.
Gomez C, Kennedy B. 2018. Capturing volcanic plumes in 3D with UAV-based photogrammetry at Yasur Volcano - Vanuatu. J Volcanol Geothermal Res, 350: 84-88.
Helle RH, Lemu HG. 2021. A case study on use of 3D scanning for reverse engineering and quality control. Mater Today, 45: 5255-5262.
Javaid M, Haleem A, Pratap SR, Suman R. 2021. Industrial perspectives of 3D scanning: Features, roles and it's analytical applications. Sensors Int, 2: 100-114.
Kanun E. 2021. Using photogrammetric modeling in reverse engineering applications: Damaged turbocharger example. Mersin Photogrammet J, 3(1): 21-28.
Kingsland K. 2020. Comparative analysis of digital photogrammetry software for cultural heritage. Digital Appl

- Archaeol Cultural Herit, 18: 157.
- Kohtala S, Erichsen JF, Wullum OP, Steinert M. 2021. Photogrammetry-based 3D scanning for supporting design activities and testing in earlystage product development. *Procedia CIRP*, 100: 762-767.
- Kurilová V, Bemberáková D, Kocián M, Šterbák D, Knapčok T, Palkovič M, Hančák S. 2023. Unexpected corneal reflection phenomenon alters smartphone 3D image-based models of the eye. *J Elect Eng*, 74(6): 513-520.
- Mathys A, Semal P, Brecko J, Van den Spiegel D. 2019. Improving 3D photogrammetry models through spectral imaging: Tooth enamel as a case study. *Plos ONE*, 14(8): 1-33.
- Matthews NA. 2008. Aerial and close-range photogrammetric technology: providing resource documentation, interpretation, and preservation. US Department of the Interior, Bureau of Land Management, National Operations Center, Denver, Colorado, US.
- Molnár A. 2019. Surveying archaeological sites and architectural monuments with aerial drone photos. *Acta Polytech Hungarica*, 16(7): 217-232.
- Orun AB, Goodyer E, Smith G. 2018. 3D non-invasive inspection of the skin lesions by close-range and low-cost photogrammetric techniques. *Image Analy Stereol*, 37(1): 63-70.
- Pepe M, Costantino D. 2020. UAV photogrammetry and 3D modelling of complex architecture for maintenance purposes: The case study of the Masonry Bridge on the Sele River, Italy. *Period Polytech Civil Eng*, 65: 1-13.
- Puerta APV, Jimenez-Rodriguez RA, Fernandez-Vidal S, Fernandez-Vidal SR. 2020. Photogrammetry as an engineering design tool. In Alexandru C, Jaliu C, Comșit M eds., *Product design*, IntechOpen, London, UK, pp: 41.
- Reis HC. 2018. Detection of foot bone anomaly using medical photogrammetry. *Int J Eng Geosci*, 3(1): 1-5.
- Remondino F, El-Hakim S. 2006. Image-based 3D modelling: A review. *Photogrammet Record*, 21(115): 269-291.
- Rues S, Waldecker M, Rammelsberg P, Zenthöfer A. 2021. Effect of mesh homogeneity and choice of target surface on statistical evaluation of mesh differences. *Biotribology*, 1(26): 100-176.
- Seeberger R, Hoffmann J, Freudlsperger C, Berger M, Bodem J, Horn D, Engel M. 2016. Intracranial volume (ICV) in isolated sagittal craniosynostosis measured by 3D photocephalometry: A new perspective on a controversial issue. *J Cranio-Maxillofacial Surg*, 44(5): 626-631.
- Slaker B, Mohamed K. 2017. A practical application of photogrammetry to performing rib characterization measurements in an underground coal mine using a DSLR camera. *Int J Mining Sci Technol*, 27(1): 83-90.
- Struck R, Cordoni S, Aliotta S, Pérez-Pachón L, Gröning F. 2019. Application of photogrammetry in biomedical science. In: Rea P (eds) *Biomedical Visualisation. Advances in Experimental Medicine and Biology*, vol 1120. Springer, Cham, pp: 121-130. https://doi.org/10.1007/978-3-030-06070-1_10
- Surmen HK, Akalan NE, Fetvaci MC, Arslan YZ. 2018. A Novel dorsal trimline approach for passive-dynamic ankle-foot orthoses. *Strojniški Vestnik J Mechan Eng*, 64(3): 185-194.
- Surmen HK. 2023. Photogrammetry for 3D reconstruction of objects: Effects of geometry, texture and photographing. *Image Analy Stereol*, 42(2): 51-63.
- Tóth D, Petrus K, Heckmann V, Simon G, Poór VS. 2021. Application of photogrammetry in forensic pathology education of medical students in response to COVID-19. *J Forensic Sci*, 66(4): 1533-1537.
- Valinasab B, Rukosuyev M, Lee J, Ko J, Jun MBG. 2015. Improvement of optical 3D scanner performance using atomization-based spray coating. *J Korean Soc Manufact Technol Eng*, 24(1): 23-30.
- Wang H, Zhou J, Zhao T, Tao Y. 2016. Springback compensation of automotive panel based on three-dimensional scanning and reverse engineering. *Int J Advan Manufact Technol*, 85(5): 1187-1193.
- Yaman A, Yılmaz HM. 2017. The effect of object surface colors on terrestrial laser scanners. *Int J Eng Geosci*, 2(2): 68-74.
- Yang S, Shi X, Zhang G, Lv C. 2018. A dual-platform laser scanner for 3D reconstruction of dental pieces. *Engineering*, 4(6): 796-805.